A systematic study of polarons due to oxygen vacancy formation at the rutile TiO_2(110) surface by GGA + *U* and HSE06 methods

2012 J. Phys.: Condens. Matter 24 435504

(http://iopscience.iop.org/0953-8984/24/43/435504)

IOP PUBLISHING JOURNAL OF PHYSICS: CONDENSED MATTER

J. Phys.: Condens. Matter **24** (2012) 435504 (8pp) doi:10.1088/0953-8984/24/43/435504

A systematic study of polarons due to oxygen vacancy formation at the rutile TiO_2(110) surface by GGA + U and HSE06 methods

Taizo Shibuya[1], **Kenji Yasuoka**[1], **Susanne Mirbt**[2] **and Biplab Sanyal**[2]

[1] Department of Mechanical Engineering, Keio University, Yokohama 223-8522, Japan
[2] Department of Physics and Astronomy, Uppsala University, Box 516, SE-75120 Uppsala, Sweden

E-mail: Biplab.Sanyal@physics.uu.se

Received 16 April 2012, in final form 10 August 2012
Published 3 October 2012
Online at stacks.iop.org/JPhysCM/24/435504

Abstract

The polaronic nature of excess electrons accompanying an oxygen vacancy in a TiO_2(110) surface has been studied by several theoretical approaches. According to previous studies, DFT + U and hybrid functional methods predict different sites of localization of the polarons. In this paper, we conducted a thorough comparison of the results obtained by GGA + U (generalized gradient approximation + Hubbard U) and HSE06 (Heyd–Scuseria–Ernzerhof hybrid functional) approximations. Considering initial symmetry breaking in the geometry optimization process, we show that regardless of the approximations used, electrons localize at two particular subsurface Ti sites in a state with mixed $d_{x^2-y^2}/d_{z^2}$ character in the global coordinate frame with a spatial extent of the order of 7 Å. The lowest state of the polarons is a singlet, but the triplet is only about 0.1 meV higher in energy. Our results agree with previous experiments and calculations, wherever available. We stress that the hybrid functional has been first applied on this surface with a realistic coverage of oxygen vacancies corresponding to the experimental situation (∼12.5%).

(Some figures may appear in colour only in the online journal)

1. Introduction

TiO_2 is a functional material with widespread applications in technology [1]. Its wide bandgap (3 eV) is, for example, utilized in sunscreening and chemical solar cells. Also it is used in photocatalytic splitting of water [2] and degradation of organic molecules in polluted air or water. TiO_2 crystallizes in three phases: anatase, rutile, and brookite. The most stable bulk phase is rutile and the most stable surface is the (110) rutile surface followed by the (101) anatase surface [3]. The geometric structure of the most stable defect free (110) rutile surface has been studied both experimentally and theoretically [4] and is generally agreed to be the (1 × 1) surface with bridging oxygen rows [5].

Experimentally, the broad bandgap state at ∼1 eV below the conduction band edge has been associated with the occurrence of oxygen vacancies accompanied by the presence of Ti^{3+} ions: ultraviolet photoemission spectroscopy (UPS), resonant photoemission, electron energy loss spectroscopy (EELS) and x-ray photoelectron spectroscopy (XPS) all attribute the ∼1 eV state to Ti^{3+} ions [6]. Recently it was proposed that the bandgap state at ∼1 eV below the conduction band edge is not caused by the oxygen vacancy but by Ti interstitial defects [9], but these results are under debate [10, 12, 11].

Recent reviews of the current understanding of oxygen vacancies at the TiO_2 surface summarize both experimental [4] and theoretical results [6, 7]. Substantial experimental evidence exists to show the presence of bridging oxygen vacancies on the rutile TiO_2(110) surface. Their concentration is reported as several per cent: 8% for a surface annealed in vacuum [8], (4 ± 0.6)% [10] and ∼15% [35] for a surface

prepared by cycles of Ar bombardment and annealing. In most experimental studies, an oxygen vacancy concentration of roughly 10% is reported [4].

Calculations based on local density approximations (LDA) or generalized gradient approximations (GGA) to the density functional theory (DFT) are insufficient for systems with strong electron correlations. In addition, both LDA and GGA calculations are known to severely underestimate oxide bandgaps due to the built-in self-interaction error. Within LDA/GGA, the bandgap state corresponding to the oxygen vacancy is calculated to be at the bottom of the conduction band [6], which is in disagreement with experiment.

To overcome this problem, both GGA + U [13–16] and hybrid functional [17, 18] approaches have been conducted, where a Ti^{3+} state is reported with the presence of a gap state. This state corresponds to one localized electron, which is trapped by a local lattice distortion around a Ti ion, i.e. a polaron. But the location of the polarons varies in different calculations. Some have reported two surface polarons [17], some two equivalent polarons on subsurface sites [15, 16] and others a combination with a sub-subsurface polaron and a subsurface polaron [14].

The localization of the electrons can be achieved by either employing the DFT + U (LDA + U/GGA + U) method or a hybrid functional. Within the quantum chemistry community, the B3LYP hybrid functional is rather common and is used to cure the above-mentioned errors of the local density approximation regarding the approximate description of the electron–electron interaction. The B3LYP consists of a weighted sum over the exact exchange according to Hartree–Fock and density functional exchange–correlation, where the weights are parameters. The disadvantage is that the correlation in the limit of the homogeneous electron gas is not correctly described [27] and it is often worse than HSE06 in describing ground state properties, especially of inorganic solids [25]. In this work we use instead, as hybrid functional, the HSE06 functional. It has been shown to describe the lattice and electronic properties of TiO_2 in very good agreement with experiment [26].

A computationally inexpensive way of treating the problem is by the GGA + U method. GGA + U consists of the GGA exchange–correlation functional plus a Hubbard U term which is weighted by the orbital and spin occupation. In addition, some part of the GGA exchange/correlation functional has to be subtracted in order to minimize the double counting. The usage of GGA + U on TiO_2 does not correct the bandgap: the bandgap becomes 2.2 eV compared to an experimental bandgap of 3 eV, but allows for the electron localization at Ti ions.

A systematic comparison between these two approaches is missing in the literature. In this paper we present a thorough comparison between DFT + U and hybrid functional results of the polaron formation due to the presence of oxygen vacancy on the (110) rutile TiO_2 surface. Comparing HSE06 and GGA + U, the HSE06 functional shows overall better agreement with experimental values available for TiO_2. At the same time the HSE06 functional is computationally more expensive. By comparing HSE06 with GGA + U we want to determine if the polaron formation in TiO_2 is described sufficiently accurately by using GGA + U. We analyze our results in terms of local lattice distortions, charge distribution around polarons and magnetic exchange interactions between the polarons.

2. Computational methods

For DFT calculations, we used a plane wave based pseudopotential code, VASP [19]. The exchange–correlation potential was approximated within the generalized gradient approximation by the Perdew–Becke–Ernzerhof (PBE) [20] method and for some calculations with PW91 [21].

For the GGA + U calculation, we used PBE and an effective value of the Coulomb parameter U ($U_{\text{eff}} = U - J =$ 4.2 eV, J being intra-atomic exchange parameter) in the Dudarev approach, following Deskins *et al* [15]. We used a fixed value of U_{eff} and did not investigate the dependence of the polaron formation on the value of U as has been done by Deskins *et al* [15]. They have found that the values of U_{eff} between 3.3 and 5.4 eV do not influence the relative energies among possible polaron sites, but only change the position of the polaron state within the bandgap.

For the hybrid functional calculations, we chose the screened hybrid functional of Heyd, Scuseria, and Ernzerhof (HSE06) [22], where correlation is described in GGA (PBE) and the exchange is a mixture of 25% exact (HF) exchange and 75% PBE exchange. The advantage of this hybrid functional is that it is numerically feasible due to its mixing of only the short-ranged interaction. Moreover, the correlation is described correctly in the limit of the homogeneous electron gas. The HSE06 has successfully been tested on many materials' ground state properties, including the bandgap [24, 25]. Especially, the HSE06 functional has been used by Janotti *et al* [26] for studying oxygen vacancies in bulk rutile TiO_2, where they found the HSE06 functional to improve the agreement between the calculated ground state properties and the experimental results.

Due to the high computational cost of hybrid functionals in general, we restricted our supercell size. The surface was modeled by a p(4 × 2) geometry with a slab thickness of 4 layers separated by 10 Å vacuum. This amounts to 128 oxygen and 64 titanium ions. We have modeled the TiO_2 surface by a 6-layer slab with pseudohydrogen termination and 20 Å vacuum, a 9-layer slab with two surfaces and 20 Å vacuum, and a 4-layer slab with 10 Å vacuum. In terms of the qualitative description of the ideal surface reconstruction, the lattice relaxation due to the oxygen vacancy, the vacancy formation energy and the work function, the used slab models show agreement between each other.

We used lattice constants of $a = 4.647$ Å and $c =$ 2.983 Å, which were determined by the calculations for bulk TiO_2. For the surface calculations, the bottom layer was fixed at bulk positions and terminated by pseudohydrogen [23] atoms. The Brillouin zone was sampled by a 2 × 2 × 1 Monkhorst–Pack grid unless stated otherwise. The plane wave cut-off energy was 450 eV and the core–valence interaction

was described by the projector augmented wave approach (PAW).

We find in agreement with earlier calculations [13] that the relaxed polaron structure strongly depends on the initial structure. According to need, we adopted the following three schemes to localize an electron at the targeted site. The starting structure of those schemes was always the optimized surface structures by PW91. In all schemes, we removed one O atom in the beginning of the simulations. Unless otherwise stated, the calculations were performed in spin-polarized mode.

Scheme 1: first we chose two Ti sites at which we aimed to localize an electron. Then we substituted that Ti with a V atom and let the surface to relax. After that we recovered that site and relaxed it again. This corresponds to the procedure of Deskins *et al*.

Scheme 2: first we chose two Ti sites and expanded the distance to the neighboring oxygen atoms by 5%. Then we allowed the surface to relax. This is according to Chrétien *et al* [14].

Scheme 3: first we relaxed the surface with a restriction of non-spin polarization. Then we followed scheme 2.

In order to investigate the triplet and singlet states, when needed, we posed an extra restriction which fixed the total magnetic moment at either 0 or 2 μ_B. In all cases, Hellmann–Feynman forces were reduced until 0.05 eV $Å^{-1}$.

3. Results and discussions

3.1. Ideal surface reconstruction

The ideal rutile TiO_2 structure has an orthorhombic D_{2h} symmetry, because not all 6 oxygen–titanium bonds are equal [28]. The (110) surface is the cleavage surface of rutile TiO_2. The surface is charge neutral and reconstructs in a (1 × 1) pattern. It contains both Ti and O ions with two different coordinations: the outermost ions are two-fold coordinated oxygen ions located in a bridge position (see figure 1). This oxygen row is called the bridging oxygen row. The bridging oxygen ions are located on top of six-fold coordinated Ti ions. These Ti ions form a row, which we will call the Ti6c row. The Ti6c ions are oriented such that the plane containing its four oxygen neighbors is perpendicular to the surface along the Ti6c row. Between two surface Ti6c rows lies a five-fold coordinated Ti row, which we will call the Ti5c row. The Ti5c row is oriented such that the plane containing its four oxygen neighbors is parallel to the surface. The oxygen ($O_{\text{in plane}}$) in between Ti6c and Ti5c rows is three-fold coordinated.

Electron counting [32] gives that every surface Ti5c ion contributes 2/3 electrons less to its bonds than its valency. This implies that every Ti5c ion is charged with +2/3 electrons. At the same time the surface Ti6c ion is charged with −2/3 electrons. The charge transfer between Ti5c and Ti6c surface ions makes the (110) surface charge neutral. The positive charge on the surface Ti5c ion increases the ionicity of the Ti5c–O bonds due to which the surface Ti5c–$O_{\text{in plane}}$ bond lengths decrease by 0.6%. The opposite happens for the Ti6c–$O_{\text{in plane}}$ bonds: the negative charge on the surface Ti6c ions decreases the ionicity of the surface Ti6c–$O_{\text{in plane}}$ bonds, due to which the bond lengths are increased by 2.6%.

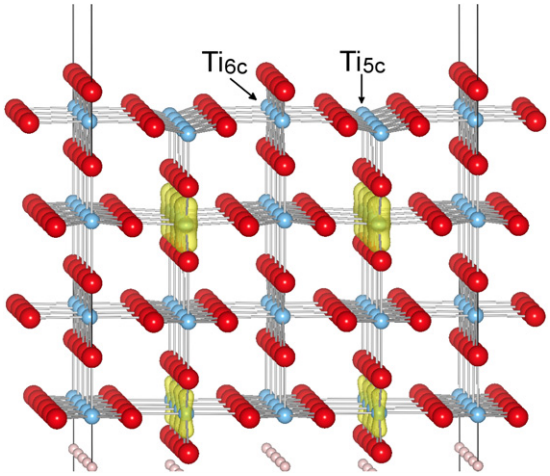

Figure 1. Charge density of the lowest unoccupied state of a defect free TiO_2 (110) surface. Dark circle (red): oxygen, light circle (blue): titanium.

Our calculated lowest unoccupied state has a b_{2g} character (d_{xz}) for bulk TiO_2. The lowest unoccupied state of the ideal rutile TiO_2(110) surface is located on the Ti ions below the surface Ti5c rows (see figure 1) and is a mixture of 90% d_{z^2} and 10% $d_{x^2-y^2}$ character in the global coordinate frame. The surface Ti5c states are located about 0.15 eV (0.12 eV with PBE + U) higher up in energy. We calculate the work function to be 7.9 (6.9) eV within HSE06 (PBE).

Comparing the ideal surface reconstruction patterns, we find a difference between PBE + U and HSE06. In table 1 we compare the displacement of the ions relative to the positions of the ideal cleaved surface. The buckling of the surface is reproduced independent of the exchange approximation used here. In PBE, PBE + U and HSE06 we get a buckling of 0.4 Å comparing the positions of a Ti6c and a Ti5c ion, which is in excellent agreement with experiments (see the last columns in table 1). But with HSE06 the overall displacement of the ions is an inward relaxation, whereas with PBE + U it is an outward displacement. This is best reflected considering the relaxation of the bridging oxygen ion: In PBE + U it moves 0.24 Å out of the surface, in PBE it more or less stays in the surface, whereas in HSE06 it moves into the surface. Unfortunately, the two experiments deviate in the displacement of the bridging oxygen ion: with LEED it is measured to move out of the surface whereas with SXRD it is measured to move into the surface. Overall, the LEED results agree better with the PBE+U calculations, whereas the SXRD results agree better with the HSE06 results. In summary, with HSE06 (PBE + U) the bond between Ti6c and the bridging oxygen ion becomes stronger (weaker), in agreement with the SXRD (LEED) results. Future experiments must clarify this issue.

Table 1. Ionic displacement in (Å) within the relaxed surface relative to the ideal cleaved surface.

	PW91 [29]	FLAPW [30]	PW91 (this work)	PBE + U (this work)	HSE06 (this work)	SXRD [31]	LEED [5]
Ti6c	0.21	0.08	0.21	0.37	0.1	0.12 ± 0.05	0.25 ± 0.03
Ti5c	−0.21	−0.23	−0.18	0.03	−0.26	-0.16 ± 0.05	-0.19 ± 0.03
O_{bridge}	0	−0.16	0.03	0.24	−0.1	-0.27 ± 0.08	0.10 ± 0.05
$O_{in\ plane}$	0.14	0.09	0.16	0.36	0.05	0.05 ± 0.05	0.27 ± 0.08
$Ti_{below\ Ti6c}$	0.13	0.07	0.16	0.24	0.07	0.07 ± 0.04	0.14 ± 0.05

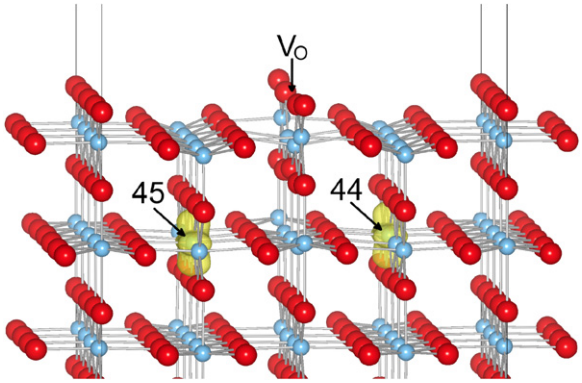

Figure 2. Charge density of the energetically lowest polaron state of a oxygen vacancy containing TiO_2(110) surface. Isosurface level = 0.015 e Å^{-3}. Dark circle (red): oxygen, light circle (blue): titanium.

3.2. Oxygen vacancy formation

The optimized lattice structure with an oxygen vacancy after the removal of one bridging oxygen ion at the surface is shown in figure 2. In the following, we call the two Ti ions in the surface Ti6c row neighboring the vacancy, Ti6c*. These ions are located in the Ti6c row but have become five-fold coordinated due to the vacancy formation. An oxygen vacancy in bulk TiO_2 gives rise to an excess of two electrons because the removal of one oxygen ion leaves 3 partially filled (with 2/3 electrons each) dangling bonds on its Ti neighbors. An oxygen vacancy in the surface layer also gives rise to an excess of two electrons, because the removal of a two-fold coordinated oxygen ion leaves two partially occupied Ti dangling bonds (with 1 electron each). Due to the missing oxygen ion, a local reconstruction of the vacancy neighbors occurs. In the following, the relaxation patterns obtained by HSE06 (PBE + U) are provided. The oxygen ion below the two Ti6c* ions moves up by 2.2 (1.1)% and the Ti6c* ions move down by 2.6 (2.2)%. This gives rise to a Ti–O–Ti bond angle of 126° (116°) compared to 90° for an octahedral configuration. The bond length between Ti6c* and the underlying oxygen ion (called O164 in the following) is reduced by 2.1% compared to the bulk value whereas the bond between O164 and the underlying Ti ion (called Ti36 in the following) is increased by almost 22 (11)%.

Electron counting reveals that the surface cannot remain semiconducting by only rearranging the electrons on the Ti–O bonds. (It would leave partially occupied dangling bonds on some Ti ions.) Instead the two excess electrons are localized on two Ti ions (see section 3.3), which preserves the semiconducting properties of TiO_2, because no partially occupied state arises. Since the surface is charge neutral, an excess of two electrons implies that somewhere in the surface a charge of +2 exists. Again electron counting shows where the charge of +2 is located: one Ti ion in the Ti5c row remains holding +2/3 electrons, which now is not compensated by a bridging oxygen due to the absence of one oxygen ion. The additional charge of +4/3 electrons is located on the Ti6c* ions, on each Ti6c* ion a charge of +2/3.

3.3. Polaron formation

TiO_2 is an ionic semiconductor. For ionic semiconductors the bandgap increases with increasing degree of ionicity and vice versa. The oxygen (titanium) sites are charged with −2 electrons (+4 electrons), in short [O(−2); Ti(+4)]. The system can gain energy by localizing the excess electrons on two equivalent Ti ions: localizing one electron on a Ti ion [O(−2); Ti(+3)] will locally lower the ionicity. This Ti ion is attracted less by its oxygen neighbors. Its bond lengths and the volume of the local octahedron centered on this Ti ion are increased. In addition, a lowering of the ionicity is equivalent to a lowering of the energy eigenstates.

In the ideal rutile lattice the two excess electrons can only populate the conduction band, because the valence band is completely occupied. The site projection of the ideal structure's lowest unoccupied state is shown in figure 1. The electron localization is equivalent to a spatial symmetry breaking of this state, where this state is shared now by only two Ti ions. This electron localization accompanied by a local lattice distortion is termed a polaron.

The energetically most stable solution of the two polarons obtained by us is in agreement with earlier calculations [15, 16]. The polaron is in the subsurface layer below the Ti5c rows (see figure 2). This configuration is called 44–45 in the following discussions. Comparing figures 1 and 2 one clearly sees the spatial symmetry breaking. This explains why the polarons are located in the subsurface layer. The polaron state is a mixture of 84% d_{z^2} and 16% $d_{x^2-y^2}$ character within HSE06 and 80% d_{z^2} and 20% $d_{x^2-y^2}$ character within PBE+U in the global coordinate frame.

In figure 3 we show the calculated density of states of the (110) surface with one oxygen vacancy. We calculate the vacancy to be accompanied by a polaron state 1.22 eV (1.50 eV with PBE + U) below the conduction band edge. The bandgap at the Γ-point is calculated to be 3.19 eV with HSE06 and 2.11 eV with PBE + U.

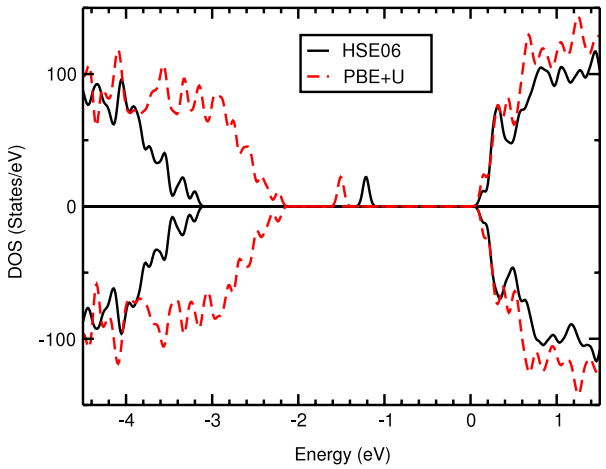

Figure 3. Density of states of the oxygen vacancy. Solid (red dashed) line is for HSE06 (PBE + U) results. The conduction band edges in these two methods have been aligned.

In figure 4 we show the charge density of the polaron state. Both PBE + U (right figure) and HSE06 (left figure) give more or less the same spatial distribution of the polarons. The polaron is 72% located on the center Ti site and the remaining 28% is spread out on its oxygen and mainly titanium neighbors, as is shown in figure 4. The polaron shape follows the symmetry of the on-site d-orbital. It is thus more or less contained within the plane containing the four neighboring oxygen ions. In the direction of the Ti rows the polaron has a size of about 6 Å, and in the direction perpendicular to the Ti row it has a size of about 7 Å. This is in good agreement with recent electron transport measurements by Hendry *et al* [33], where they fitted their results to the Feynman polaron model and obtained a polaron radius between 4 and 8 Å, depending on their choice for the optical-phonon coupling constant.

The polaron formation gives rise to an increase in the bond length between the Ti ion and its O neighbors by ∼0.1 Å per bond, but only for the bonds in the plane of the four oxygen ions around the polaron center ion. This anisotropy of the polaron geometry reflects the shape of the state with mixed $d_{x^2-y^2}/d_{z^2}$ character in the global coordinate frame (figure 4) and explains the quasiplanar shape of the polaron. The bond length in the perpendicular direction is not altered compared to the bulk. The volume of the octahedron connecting the nearest neighbors of the Ti center ion is increased by 11% within HSE06 and by the same amount in PBE + U calculations due to the polaron formation.

In order to investigate the difference between PBE + U and HSE06, we show in the bottom of figure 5 the charge density of the HSE06 polaron state minus the PBE+U polaron state. (As the lattice relaxation is different between PBE + U and HSE06, we first recalculated the charge density within PBE + U, but using the HSE06 relaxed lattice positions. The charge density obtained in this way looked identical to the right panel in figure 4, i.e. we see no difference in the charge density using the HSE06 or PBE+U lattice positions.) Within PBE + U we calculate the charge to be larger close to the center Ti ion (white) and smaller on the Ti neighbors (green). This indicates that PBE+U overestimates the electron localization.

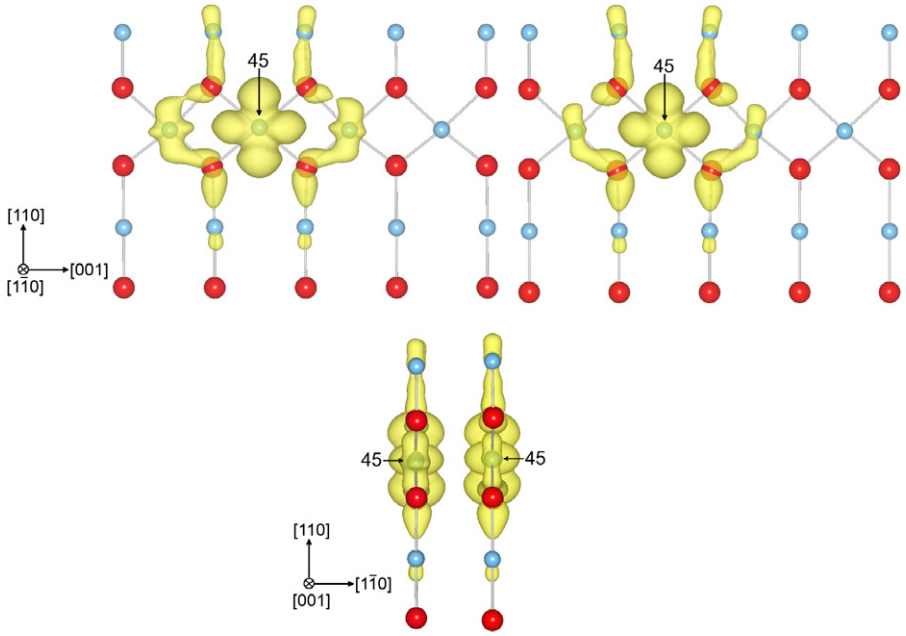

Figure 4. Charge density of the polaron state. Isosurface level is 0.0013 e Å^{-3}. (Top panel) Side-view along [001] direction. Left (right) panel HSE06 (PBE + U). (Bottom panel) Side-view along the [1$\bar{1}$0] direction. Left (right) panel HSE06 (PBE + U). Readers are referred to figure 2 to identify the location of oxygen vacancy.

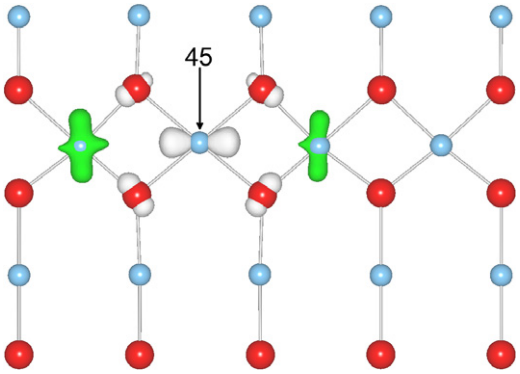

Figure 5. Polaron charge density difference: HSE06–PBE + U. White indicates 'negative' and green indicates 'positive'. Isosurface level is 0.0013 e Å^{-3}. Readers are referred to figure 2 to identify the location of oxygen vacancy.

Table 2. Polaron energy in (eV) for different polaron sites.

	PBE+U [14]	DFT+U [15]	PBE+U [16]	PBE+U (this work)	HSE06 (this work)
44–45	0	0	0	0	0
44–46	0	0.06	—	0.28	0.28
38–44	0	0.23	0.22	0.23	0.27
38–52	0.3	0.96	—	—	0.90

3.4. Polaron site

The final sites of the polarons are strongly dependent on the initial volume expansion. If we calculate the oxygen vacancy containing surface without initial local volume distortions, we find a solution with two polarons, one residing in the subsurface layer below the Ti6c* ion and one in the surface layer on Ti6c*. In the following we call this configuration 38–52 (see figure 6). It is 0.9 eV higher in energy than the lowest energy configuration (see table 2). (The polaron state centered on the Ti6c* ion is 0.5 eV below the conduction band compared to 1.2 eV for the subsurface polaron state.) In agreement with this calculation, Di Valentin *et al* [17] did not vary the initial polaron positions and only found two polarons in the surface layer.

Providing an initial volume expansion (as referred to scheme 2 above) around two arbitrary Ti ions still does not lead to the energetically lowest polaron configuration. Instead we find a solution where both polarons are in the subsurface layer, one below the Ti5c row and the other below the oxygen vacancy. In the following, this configuration is called 38–44 (see figure 6). It is 270 meV higher in energy (see table 2) and has two polaron peaks in the bandgap. The spatial extension of the polaron is identical to the 44–45 configuration shown in figure 4 with the exception of the orientation: the polaron lying below the oxygen vacancy has its charge distributed mainly in a plane perpendicular to the polaron shape of configuration 44–45. This polaron shape is mainly contained in a plane parallel to the surface, because the central Ti ion has its four oxygen neighbors in a plane parallel to the surface (see figure 6). Since the state below the oxygen vacancy is not a part of the defect free unoccupied state (see figure 1) the 38–44 configuration has to be higher in energy than the 44–45 configuration. Also, we find a polaron in the third layer below the surface to be unstable. Only when either initially replacing two Ti ions with V as proposed by Deskins *et al* [15] (as referred to scheme 1 above) or completely relaxing the oxygen vacancy before allowing for polaron formation (as referred to scheme 3 above), we find the lowest polaron configuration 44–45 in agreement with Deskins *et al* [15] and Kowalski *et al* [16]. This indicates that the energy barrier of this 44–45 configuration is rather large. If the oxygen vacancy is not formed in advance, enlarging the oxygen cage around the polaron centers of configuration 44–45 does not lead to the 44–45 configuration but always go back to the 38–44 configuration.

In table 2, we compare the relative energies of different polaron configurations calculated by different methods. One sees that the relative energy difference calculated by PBE + U or HSE06 gives more or less identical results. Only for the second row, configuration 44–46, is there a difference between Deskins *et al* [15] and our PBE + U results, whereas our PBE + U and HSE06 results are similar.

Configuration 44–46 consists of both polarons within the same Ti row in the subsurface layer (see figure 6). Both polarons are located below the same Ti5c row and are neighboring each other. This polaron state is a mixture of 77% d_{z^2} and 23% $d_{x^2-y^2}$ character within HSE06 and of

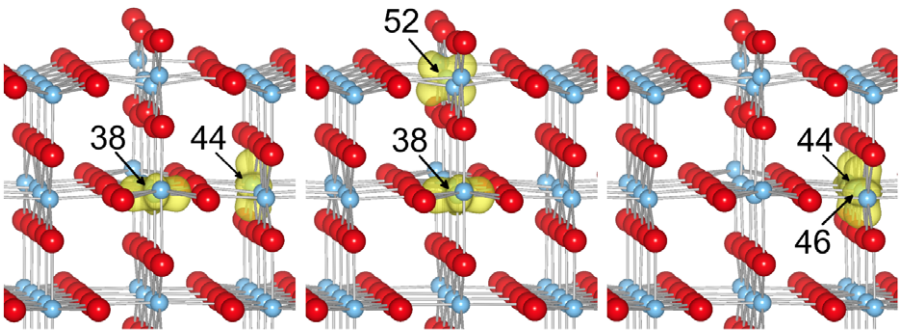

Figure 6. Charge density of the polaron state for three different polaron geometries as described in the text. Isosurface level is 0.015 e Å^{-3}.

70% d_{z^2} and 30% $d_{x^2-y^2}$ character within PBE + U in the global coordinate frame. We find this configuration to be 0.28 eV higher in energy, whereas Deskins *et al* found it only 0.06 eV higher. We believe this difference to be caused by the following.

In one inset (see figure 2 in [15]) Deskins *et al* showed the spin density of their polarons. As can be seen, one polaron has its extension in the plane of the four neighboring oxygens (blue color), but the other polaron has its extension in a plane perpendicular to the plane of the four oxygen neighbors. In the 44–46 configuration, the two polarons are neighbors, which implies that their charge density is slightly overlapping. (The polaron is mainly contained in the plane perpendicular to the Ti5c row and to the surface.) In our calculations, the two polarons in the 44–46 configuration consist of identical orbitals, whereas in the calculations of Deskins *et al* [15], it seems that the two polarons consist of two orthogonal orbitals. Therefore the spatial overlap of the two polarons in configuration 44–46 will cost more in our calculation than in their calculation. The two polarons in configuration 44–46 having orthogonal states is in contradiction with both our calculations and our interpretation of the polaron formation. Therefore we suspect that this difference might be related to the different basis set (Gaussian) in their calculation. This difference is important because if Deskins *et al* are correct about the 44–46 configuration being energetically so close to the lowest 44–45 configuration, then in experiment both configurations should be seen. If our calculations are correct, in experiment only configuration 44–45 should be seen. Further calculations and experiments must shed light on this question.

A polaron containing two electrons on the same site is found to be unstable. This we conclude from a calculation with a (2 × 1) unit cell where only one ion initially was distorted, but we do not get a solution with one ion being doubly occupied. This indicates that the on-site Coulomb repulsion between two d-electrons is larger than the energy difference between the singly occupied polaron state and the conduction band edge, i.e. larger than 1.2 eV.

Krüger *et al* [34] used resonant photoelectron diffraction to probe defect states at the rutile TiO_2(110) surface. They conclude that a substantial part of the probed defect charge is located on subsurface layers, with a maximum on the subsurface Ti ion located below the Ti5c row. They find a negligible charge of the subsurface Ti ion below the Ti6c row. They find the surface layer sites Ti6c* and Ti5c to carry a small, but non-negligible amount of charge. These experimental findings rule out Di Valentins [17] calculations but confirm our, Kowalskis [16], and Deskins [15] results, because they only find polarons on Ti ions located below the Ti5c row.

Yim *et al* [10] employed STM and photoemission spectroscopy to investigate the origin of the bandgap state on the rutile TiO_2(110) surface. They measure the bandgap state to be located at about 0.9 eV below the conduction band edge, with a width on the order of about 0.5 eV, and establish that the bandgap state originates from bridging oxygen vacancies and not, as has been proposed [9], by Ti interstitial defects.

Table 3. Energetics of magnetic structures in (eV).

	AFM	FM
44–45	0	10^{-4}
44–46	0.28	0.30
38–44	0.270	0.278

The location and width of the bandgap state is in agreement with our calculations (see figure 3).

In our calculations, both parallel and antiparallel spin configurations are found out to be stable, whereas a nonmagnetic polaron configuration is unstable. In table 3, we show the calculated energy differences. Lowest in energy is the antiparallel spin configuration with a total moment of 0 μ_B. Only 0.1 meV higher we find a parallel spin configuration with a total moment of 2 μ_B. The nonmagnetic solution, where the two excess electrons are in the conduction band, we calculate to be 1 eV higher than the lowest energy configuration. In contrast to Deskins *et al* [15], our polaron states have the same symmetry independent of parallel or antiparallel spin configurations. We find the symmetry of the polaron state to be governed entirely by the orientation of the plane containing the polaron center and its four oxygen neighbors. This result we find independent of using PBE + U or HSE06.

4. Summary

In this work, we have carried out a systematic comparison between PBE + U and HSE06 methods for studying the polaron formation due to an oxygen vacancy at the rutile TiO_2(110) surface. We have found a polaron state in the bandgap, 1 eV below the conduction band edge having an energy width of about 0.3 eV. The spatial extent of each polaron is about (6.5 × 7) Å along the basal plane of the Ti centered octahedron. The two polarons are in a singlet state, but the triplet state is only about 0.1 meV higher in energy. Comparing PBE + U and HSE06, we find that for the (4 × 2) cell size PBE + U (U = 4.2 eV) and HSE06 give more or less identical relative energies. There is a difference in the relaxation pattern, but its contribution to the energy differences (relative energies) is negligible. The polaron geometry is identical for PBE + U and HSE06. The occurrence of subsurface polarons is explained in terms of spatial symmetry breaking, where the defect free unoccupied lowest state becomes localized on only two subsurface Ti sites.

Acknowledgments

Support from STANDUP is acknowledged. We also acknowledge the Swedish National Infrastructure for Computing (SNIC) for the allocation of time on high-performance supercomputers.

References

[1] Chen X and Mao S S 2007 *Chem. Rev.* **107** 2891
[2] Kudo A and Miseki Y 2009 *Chem. Soc. Rev.* **38** 253
[3] Labat F, Baranek P and Adamo C 2008 *J. Chem. Theory Comput.* **4** 341
[4] Diebold U 2003 *Surf. Sci. Rep.* **48** 53
[5] Lindsay R, Wander A, Ernst A, Montanari B, Thornton G and Harrison N M 2005 *Phys. Rev. Lett.* **94** 246102
[6] Ganduglia-Pirovano M V, Hofmann A and Sauer J 2007 *Surf. Sci. Rep.* **62** 219
[7] Pang Chi Lun, Lindsay R and Thornton G 2008 *Chem. Soc. Rev.* **37** 2328
[8] Pan J-M, Maschhoff B L, Diebold U and Madey T E 1992 *J. Vac. Sci. Technol.* A **10** 2470
[9] Wendt S *et al* 2008 *Science* **320** 1755
[10] Yim C M, Pang C L and Thornton G 2010 *Phys. Rev. Lett.* **104** 036806
[11] Wendt S *et al* 2010 *Phys. Rev. Lett.* **104** 259703
[12] Yim C M, Pang C L and Thornton G 2010 *Phys. Rev. Lett.* **104** 259704
[13] Morgan B J and Watson G W 2007 *Surf. Sci.* **601** 5034
[14] Chrétien S and Metiu H 2011 *J. Phys. Chem.* C **115** 4696
[15] Deskins N A, Rousseau R and Dupuis M 2011 *J. Phys. Chem.* C **115** 7562
[16] Kowalski P M, Canellone M F, Nair N N, Meyer B and Marx D 2010 *Phys. Rev. Lett.* **105** 146405
[17] Di Valentin C, Pacchioni G and Selloni A 2006 *Phys. Rev. Lett.* **97** 166803
[18] Minato T *et al* 2009 *J. Chem. Phys.* **130** 124502
[19] Kresse G and Hafner J 1993 *Phys. Rev.* B **47** 558
Kresse G and Furthmüller J 1996 *Phys. Rev.* B **54** 11169
[20] Perdew J P, Burke K and Ernzerhof M 1996 *Phys. Rev. Lett.* **77** 3865
[21] Perdew J P and Wang Y 1992 *Phys. Rev.* B **45** 13244
[22] Heyd J, Scuseria G E and Ernzerhof M 2003 *J. Chem. Phys.* **118** 8207
[23] Shiraishi K 1990 *J. Phys. Soc. Japan* **59** 3455
[24] Marsman M, Paier J, Stroppa A and Kresse G 2008 *J. Phys.: Condens. Matter* **20** 064201
[25] Deak P, Aradi B and Frauenheim T 2011 *Phys. Rev.* B **83** 155207
[26] Janotti A, Varley J B, Rinke P, Umezawa N, Kresse G and Van de Walle C G 2010 *Phys. Rev.* B **81** 085212
[27] Hafner J 2008 *J. Comput. Chem.* **29** 2044
[28] Brydson R, Sauer H, Engel W, Thomas J M, Zeitler E, Kosugi N and Kuroda H 1989 *J. Phys.: Condens. Matter* **1** 797
[29] Kiejna A, Pabisiak T and Gao S W 2006 *J. Phys.: Condens. Matter* **18** 4027
[30] Harrison N M, Wang X-G, Muscat J and Scheffler M 1994 *Faraday Discuss.* **114** 305
[31] Charlton G *et al* 1997 *Phys. Rev. Lett.* **78** 495
[32] Pashley M D 1989 *Phys. Rev.* B **40** 10481
Harrison W A 1979 *J. Vac. Sci. Technol.* **16** 1492
[33] Hendry E, Wang F, Shan J, Heinz T F and Bonn M 2004 *Phys. Rev.* B **69** 081101
[34] Krüger P *et al* 2008 *Phys. Rev. Lett.* **100** 055501
[35] Kappes B B, Maddox W B, Acharya D P, Sutter P and Ciobanu C V 2011 *Phys. Rev.* B **84** 161402